

On Electric Field Induced Processes in Ionic Compounds

H. Schmalzried[†]

Institut für Physikalische Chemie und Elektrochemie, Universität Hannover
 (Received September 28, 2000; Accepted April 27, 2001)

ABSTRACTS

The behaviour of ionic compound crystals under combined chemical and externally applied electrical potential gradients is discussed. Firstly, a systematic overview is given. Then a formal analysis follows. The transport equations of the ions and the electronic defects predict that even with reversible electrodes demixing, and in particular decomposition of the compound will occur if the applied d.c. current density is sufficiently high. These predictions are illustrated by appropriate experiments. With the help of the solid solution (Me, Fe)O, where Fe-ions are the dilute species, we investigate experimentally the behaviour of a ternary ionic crystal under a d.c. electric current load. All the compounds were placed in a galvanic cell, and the internal reactions which then could be observed were driven by the electric field in this cell. In addition, we discuss the influence of the electric field on the classical solid state reaction $AX+BX=ABX$, if again the reaction couple is placed in a galvanic cell.

Key words : Ionic compound, Defect, Solid state reaction

1. Introduction

The d.c.-electrical behaviour of (multicomponent) ionic compounds is given by their ionic and electronic bulk transport coefficients and the thermodynamic and kinetic coefficients established at the (phase) boundaries. The essential (isothermal) boundary conditions are: 1) Fixation of the component chemical potentials only (without electrodes). 2) Fixation of a) reversible and b) irreversible electrodes.

Since the early investigations by Tubandt, Jost and Wagner this field of problems has again and again attracted the interest of solid state physical chemists.¹⁾ Many details are still far from being understood.

In the first case (open circuit), no net electric current flows, which means that, since

$$\sum z_i \cdot F \cdot j_i = I, \quad I = 0 \quad (1)$$

(z_i = charge of species i , F = Faraday constant, j_i = flux density). Disregarding specific electrochemical processes at the electrodes for the moment being, case 2) is characterized by $I = I^0 = \text{constant}$ in the bulk of the ionic crystal in view of the fact that $\text{div } I = 0$. Before analyzing case 2) in more detail, let us briefly summarize some aspects of case 1) as the basis of chemical transport in ionic compounds. Since

$$j_i = -L_i \cdot \Delta \eta_i = -L_i \cdot \nabla (\mu_i + z_i \cdot \tilde{\phi}) \quad (2)$$

one can with the help of eq. (1) and the condition $I = 0$ eliminate the electric potential gradient $\nabla \tilde{\phi}$ in eq. (2), which yields for example for a compound AX_n with only cationic

and electronic conduction

$$j_A = -L_A \cdot t_e \cdot \nabla \mu_{A(m)} \quad (3)$$

where $\mu_{A(m)} = \mu_A$ is the chemical potential of the metal (!) component, A, and t_e is the electronic transference number defined as $t_i = z_i^2 L_i / (\sum z_i^2 L_i)$, $i = e$. (In what follows we will always deal with one ionic and one electronic flux only. In practice these are the fluxes with the highest transport coefficients. This restriction does not invalidate the generality of the discussion). Eq. 3 says that the compound AX_n exposed to a chemical potential gradient transports ions (here cations) to the extent that electrons (holes) allow for charge compensation. In semiconducting AX_n ($t_e = 1$), the metal flux is simply $j_A = -L_A \cdot \nabla \mu_A$. If $t_e = 0$, there is no mass transport.

In compound ionic crystals it is the ionic disorder (point defects) which is responsible for the ionic mobility. Therefore, in most of the cases $\mu_A + (\mu_i(\text{ion}))$ is constant in the gradient of μ_A (or μ_X), and we have in view of $\mu_A = \mu_{A^{z+}} + z_A \cdot \mu_e$

$$\nabla \tilde{\mu}_A = \nabla \mu_e \cong \nabla \tilde{\phi} \quad (t_e \approx 1) \quad (4)$$

$\nabla \tilde{\phi}$ is equivalent to a diffusion potential.

This is all well known. The scope of this investigation is different. We ask for the influence of an electric field which is externally applied if electrodes of different kind are attached to a multicomponent phase or a sequence of phases. Before treating two practically important cases in some depth, let us start by illustrating the limiting cases of chemical transport and reaction in Fig. 1.

a) Without an electric field, this is simply the permeation of the A-component across a phase sequence. If $D_X \ll D_A, D_B$, the X-sublattice (laboratory frame) is fixed. If we disregard

[†]Corresponding author

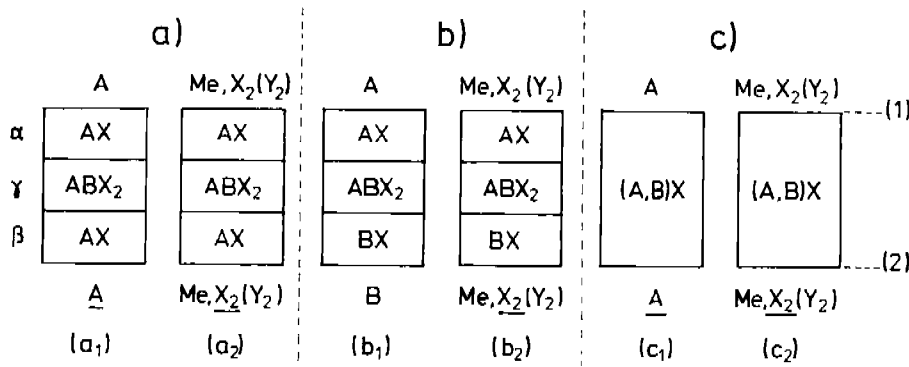


Fig. 1. Schematic overview on galvanic cells with various phase sequences which are to be studied under electrical current load

morphological instabilities of the boundaries, no changes are observed in case (a₁), whereas in case (a₂) AX will grow at the oxidizing boundary AX/Me, X₂ and will be consumed at the reducing boundary.

However, depending on the ratio $\gamma = D_A/D_B$ in ABX₂ the boundaries of the compound will move relative to the laboratory frame. If $\gamma = 0$, ABX₂ is moving relative to the laboratory frame, and if $\gamma = \infty$, ABX₂ is stationary.

b) This is the classic compound forming solid state reaction, although with the additional imposition of a chemical potential gradient. Only as long as $\mu_{X_2}(1) = \mu_{X_2}(2)$, this reaction has been fully treated.²⁾ In all other instances, additional component fluxes occur in AX and BX resulting in additional motions of the boundaries which depend on γ .

c) This illustrates the exposure of a solid solution to a chemical potential gradient with different boundary conditions. Disregarding the boundary reactions proper, assuming instead local thermodynamic equilibrium throughout, this transport problem has been treated in the literature³⁾ and is known as kinetic demixing.

Generally spoken, all the reactions of Fig. 1 are fully determined by their transport equations of the components in the respective phases and the unambiguously given boundary conditions.

In what follows we will investigate these reactions if an additional externally provided electric field is superimposed. To this end we treat two cases to some depth: 1) The behaviour of the classical solid state reaction and 2) The behaviour of a ternary solid solution such as (Mg, Fe)O under the influence of the d.c. field applied to the boundaries (1) and (2). Let us mention in passing that in principle the application of the electric field is similar to the application of other thermodynamic potential gradients, e.g. ∇P or ∇T (Ludwig-Soret-effect).

2. The Reaction Couple AX/ABX₂/BX in an Electric Field

Fig. 2 gives the two essential experimental situations in this context. The reaction $AX + BX = ABX_2$ is taking place while the phases involved are part of the electric circuit (we assume here that $D_X \ll D_A, D_B$). The constraining conditions

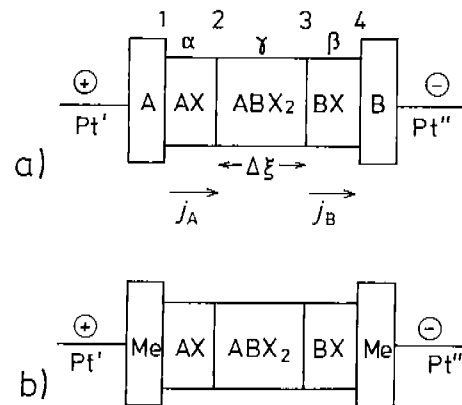


Fig. 2. Reaction couple AX/ABX₂/BX in an electric field. a) Reversible electrodes attached, b) inert electrodes attached.

is $\nabla I = 0$ or with eq. (1):

$$\sum z_i \cdot F \cdot j_i = I^0 \tag{1a}$$

This equation has to be integrated, taking into account the proper boundary conditions and using the fluxes defined in eq. (2) explicitly. From the boundary conditions we conclude:

$$j_A^\alpha = j_B^\beta = j_A^\gamma + j_B^\gamma = I^0/F = j^0 \tag{5}$$

Eq. (5) can be used to eliminate the electric potential gradient $\nabla \tilde{\varphi}$ ($F \cdot \nabla \varphi$) from the flux equations. If we now reinsert $\nabla \tilde{\varphi}$ and note that

$$1/V_{ABX_2} \cdot \frac{d\Delta \xi}{dt} = (j_A^\gamma - j_B^\gamma) \tag{6}$$

we obtain for the reaction rate

$$\frac{d\Delta \xi}{dt} = V_{ABX_2} \cdot \left\{ (t_A - t_B) \cdot j^0 - \frac{4L_A \cdot L_B}{L_A + L_B} \cdot \frac{\Delta G^0}{\Delta \xi} \right\} \tag{7}$$

From eq. (7) we can draw a number of conclusions:

1) In case of galvanic contact, the electric field influences the reaction rate through j^0 . This influence of the external field is additively superimposed to the chemical reaction proper, which is represented by the second term in eq. (7).

(t_i = transference number ; $\Delta\xi$ = thickness of ABX_2 ; ΔG° = Gibbs energy of reaction).

2) If $t_A = t_B$, the electric field has no influence on the reaction, rate, but on the displacement of the reaction layer in the laboratory frame.

3) It is possible to extend the calculations to semiconducting compounds. If $t_e \cong 1$ and $\Delta\mu_{X_2}$ between the electrodes vanishes, then there is no influence of the electric field on the reaction whatsoever. For more details see ref. [1]. Not very many experimental studies are available. Some experiments which have been performed in this context are ambiguous. The reason is that if the experiments are performed with polycrystalline material, the local current densities are inhomogeneous. This, as will be shown in the next section, may violate the condition $\nabla I = 0$. If this condition is not met, internal reactions occur and the structure of the crystals is altered. This then is the theme of the next section.

3. Effects induced by an Electric Current in Mixed Conductors (Ionic Crystals)

The experimental situation is illustrated in Fig. 1c. As an example, let us place, e.g. (Mg, Fe)O ((A, B)X) between Pt-electrodes. Under load, one has for the flux of A-ions in the semiconducting solid solution ($t_e \neq 0$) instead of eq.(3):

$$\tilde{j}_A = -L_A \cdot t_e \cdot \nabla \tilde{\mu}_A + t_A \cdot \tilde{j}^0 / z_A^2 \quad (8)$$

\tilde{j}_A is the equivalent flux, z_A is the valence of A in the crystal. As in eq. (7), the chemical and the electrical contributions to the flux are additively superimposed. Eq. (8) is again derived from the flux equations and the condition (1a) by eliminating $\nabla \tilde{\phi}$.

However, let us now also consider the case that, in view of internal demixing ($D_A \neq D_B$!), we have an inhomogeneous composition and thus t_e is locally not constant. In this case, \tilde{j}_A is not necessarily locally constant either. But in case that $\nabla \tilde{j}_A \neq 0 (= r_A)$, one has internal decomposition. From eq. (8) we then have:

$$r_A = -\nabla(L_A \cdot t_e \cdot \nabla \tilde{\mu}_A) + \nabla t_A \cdot \tilde{j}^0 / z_A^2 \quad (9)$$

Since in the extended solid solution we may approximately set $\nabla \tilde{\mu}_A \approx \nabla \mu_e$, we have in the steady state without decomposition ($r_A=0$) instead of eq. (9)

$$-\nabla(L_A \cdot t_e \cdot \nabla \mu_e) + \nabla t_A \cdot \tilde{j}^0 / z_A^2 \approx 0 \quad (10)$$

Under working conditions we may formulate that $\nabla \tilde{\mu}_A \approx \nabla \mu_e = RT \cdot \nabla \ln x_e$ so that

$$-L_A \cdot t_e \cdot RT \cdot \nabla \ln x_e + t_A \cdot \tilde{j}^0 / z_A^2 = \text{const} \quad (11)$$

and $t_e = \alpha \cdot x_e \ll 1$. Therefore,

$$\ln x_e(\xi) = f(\tilde{j}^0, L_A, T) \quad \mu_A = f(\tilde{j}^0, L_A, T) \quad (12)$$

The solution $f(\tilde{j}^0, L_A, T)$ is more complicated if $L_A = L_A(\mu_A) = L_A(\xi)$. This is the case if the diffusion coefficient depends on the component potentials of if, for example, the sample is

doped inhomogeneously. Eq. (12) tells us that $\mu_e(\xi)$ and thus $\mu_A(\xi)$ is a function of the d.c. current load. A number of publications have dealt with this problem experimentally and theoretically. Janek and coworkers and others have shown how to experimentally determine $\mu_e(\xi)$ [4,5]. For stabilized zirconia calculations have been performed on the basis of eqs. (1) and (2) to arrive at $\mu_e(\xi)$ analytically⁶⁾ with the help of an equivalent circuit.⁷⁾

If \tilde{j}^0 is chosen by the applied voltage so that $\mu_A > \mu_A^\circ$, metal A will precipitate, i.e. $r_A \neq 0$. If we neglect small changes in stoichiometry, $r_A = -\nabla j_A$ is the production of A inside the AX_n -crystal at those locations where $\mu_A(\xi) > \mu_A^\circ$. In other words, electrically driven internal chemical reactions (oxidation or reduction) are taking place.

From eq. (12) we conclude that $\mu_A(\xi) = f(\tilde{j}^0)$ and $\mu_A^\circ(\xi^*) = f(\tilde{j}^{0*}, \xi^*)$. Therefore, for $\tilde{j}^0 > \tilde{j}^{0*}$, $r_A \neq 0$ at ξ^* . Thus one has to work out r_A as a function of \tilde{j}^0 . To this end one has to know the local reaction kinetics for the A-formation (precipitation) from the reactions between the structure elements of the crystal. Without a detailed knowledge about this reaction mechanism, which is normally not available, we may in a zeroth order approach phenomenologically set for $(\tilde{j}^0 - \tilde{j}^{0*}) / \tilde{j}^{0*} \ll 1$ by linearizing:

$$r_A = k \cdot (\tilde{\mu}_A - \tilde{\mu}_A^\circ) \quad (13)$$

which would allow to solve eq. (9). However, if $(\tilde{j}^0 - \tilde{j}^{0*}) / \tilde{j}^{0*}$ is not small, then the local reaction kinetics between structure element in order to form elemental A is normally not linear in terms of μ_A (or μ_e). This has been discussed in.^{8,9)}

Any further discussion beyond this point must be specific.

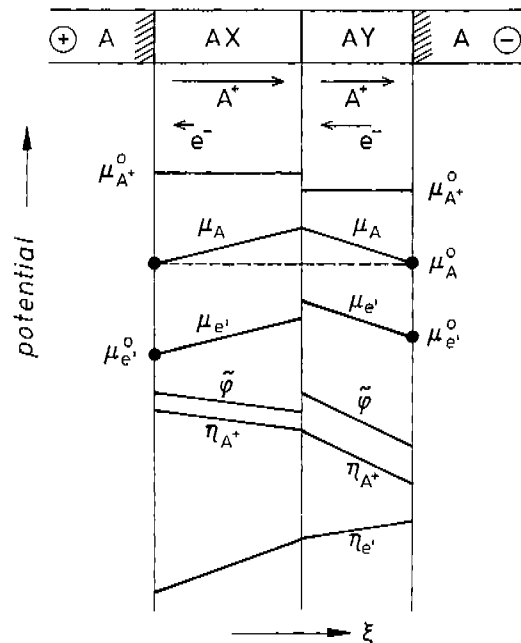


Fig. 3. The course of various thermodynamic potentials in the phase sequence A/AX/AY/A under electric load, if the transference numbers for electronic defects differ in AX and AY.

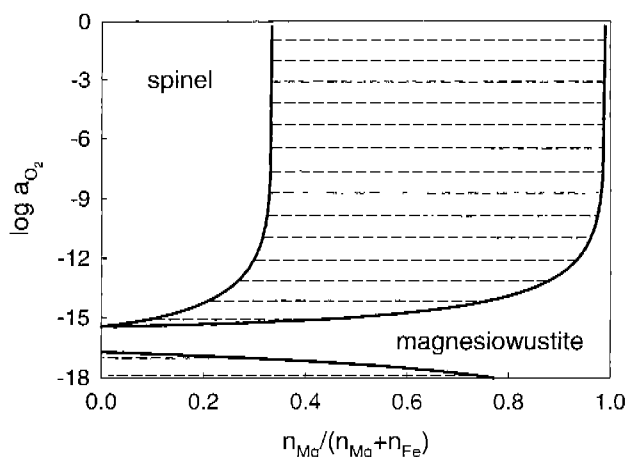


Fig. 4. Schematic phase diagram $n_{Mg}/(n_{Mg}+n_{Fe})$ vs. $\log a_{O_2}$ at $T=90^\circ\text{C}$ of the ternary system Mg-Fe-O, calculated from the equilibrium conditions of the following reactions:

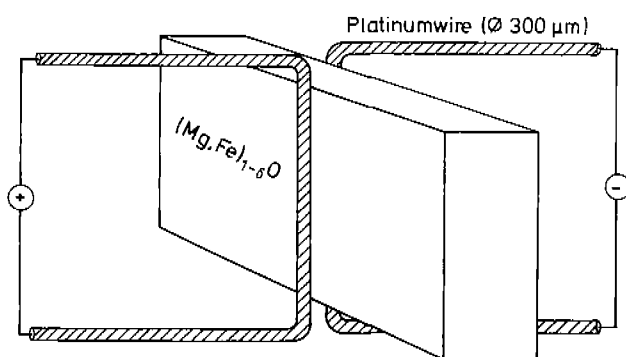
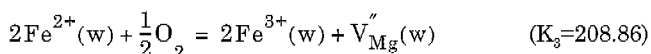
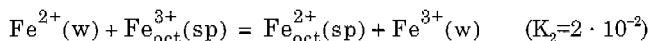
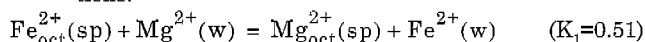


Fig. 5. Schematic plot of the geometry of the polarization cell Pt, $\text{O}_2/(\text{Mg}, \text{Fe})\text{O}/\text{Pt}, \text{O}_2$, the sample dimensions are $1900 \times 700 \times 200 \mu\text{m}^3$.

The simplest possible situation for a driven internal decomposition is shown in Fig. 3. Let us assume that the electrodes A/AX and AY/A are reversible and nonpolarizable. Instead of AY we can also use AX (doped), if doping changes the transport coefficients and the dopant is immobile. In addition let us assume that both AX and AY have a small range of homogeneity with an excess of cations (δ). Local equilibrium at the interface AX/AY means that $\mu_A^b(\text{AX}) (\equiv \mu_A^\alpha(\text{b})) = \mu_A^b(\text{AY}) (\equiv \mu_A^\beta(\text{b}))$. If $t_e^\alpha > t_e^\beta$, the calculations outlined earlier in this section yield $\mu_A^\alpha(\text{b}) = \mu_A^\beta(\text{b}) < \mu_A^0$. As long as $\mu_A(\text{b}) < \mu_A^*(\text{b})$, which is the value at which nucleation of metal A occurs at b, we may exploit eq.(11) in order to calculate $\mu_A(\xi)$ in the galvanic cell under load $j^0(I^0)$. In particular, if we know $\mu_A^*(\text{b})$, we can then calculate j^0 , i.e. the current density at which the crystals decompose by reduction at the boundary b.

Experimental investigations which resulted in internal

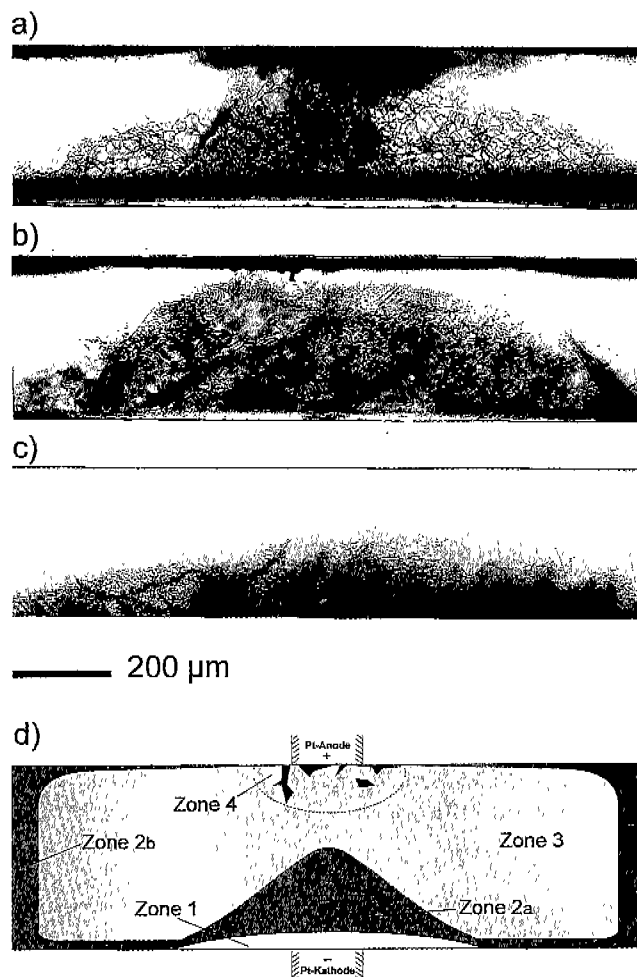


Fig. 6. Results of polarization experiments in the (Mg, Fe)O-system in air at $T=90^\circ\text{C}$ with an applied field of $E=1.5 \text{ kV}\cdot\text{cm}^{-1}$ and no preoxidation of the homogeneously doped ($x_{\text{FeO}}=1.2 \cdot 10^{-3}$) samples; cross-sections viewed by transmission optical microscopy. a) Polarization time $t=30 \text{ h}$, b) Polarization time $t=20 \text{ h}$, c) Polarization time $t=10 \text{ h}$, d) Schematic cross-section; zone 1: Fe-depleted, thin and colourless region; zone 2a: Region with spinel precipitates decorating dislocation lines due to the electrically driven internal reaction; zone 2b: Coloured region showing spinel precipitates due to the simultaneously running internal oxidation by the surrounding gas atmosphere of high oxygen activity; zone 3: No precipitates visible; zone 4: Porous area adjacent to the Pt-anode.

field driven reactions were reported in [10] and [11]. Both systems (AgBr; stabilized zirconia) are (or have been treated as) binary ones. The crucial point in the understanding of the driven chemical process inside the crystal bulk is the interplay of the various structure elements which eventually leads to the precipitation of the supersaturated component. The main theme of the rest of this paper, however, is the study of an electrically driven internal reaction in a prototype ternary system. Ternary systems are prototypes for multicomponent systems in the sense that their phase boundaries are not necessarily equipotential surfaces. They

have many practical applications, in particular oxide systems (ceramics) which are used as resistors, insulators or electrolyte material in electrical circuits. We will therefore investigate in particular the behaviour of (Mg, Fe)O in different oxygen potential atmospheres under electric load at elevated temperatures. Internal reactions in (Mg, Fe)O without application of an electric load have been studied before, e.g.¹²⁾

The crystal (Mg, Fe)O is placed between essentially irreversible Pt-electrodes, applying high voltages far beyond the decomposition voltage. Fig. 4 shows the (schematic) phase diagram of the system. Fig. 5 depicts the experimental set-up. The crystals were single-crystalline. The Fe-content was 1.2%. The experiments were performed either in air or in reducing gas atmospheres ($\text{CO}/\text{CO}_2; a_{\text{O}_2} = 10^{-8}$). A number of samples were internally oxidized^{12,16)} by keeping them sufficiently long in air at temperatures of 900 °C, before the external voltage was applied. Figs. 6-8 show typical experimental results.

The main features found are the following: If the polarization experiment is performed in air, four different zones evolve between cathode and anode, see Fig. 6. Disregarding some erratic features near the (irreversible) Pt-electrodes exposed to air, the first zone (1) near the cathode is thin and colourless. The next zone (2) is red-brownish coloured. In the inside of this zone spinel precipitates decorate dislocation lines and small angle grain boundaries. The third zone is again almost colourless. It becomes smaller the more the second zone grows with time, but it is normally found even

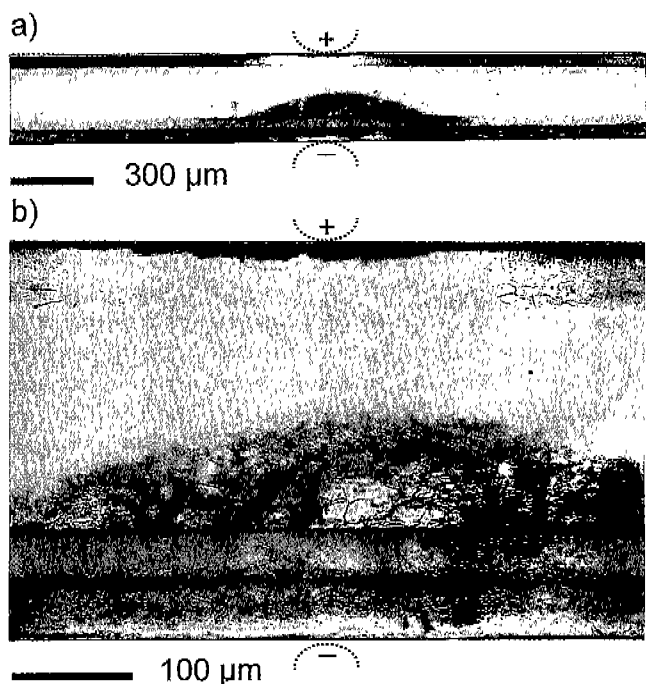


Fig. 7. Cross-section viewed by transmission optical microscopy; the polarization experiment (air, $T=900^\circ\text{C}$, $E=1.5 \text{ kV}\cdot\text{cm}^{-1}$, $x_{\text{FeO}}=1.2\cdot 10^{-2}$) has been performed after a pre-oxidation time of 100 h in air at $T=900^\circ\text{C}$.

after very long times. The fourth zone is dark brown and irregular in form, it is adjacent to the anode.

If the experiments are performed in a strongly reducing atmosphere, the tendency for internal reactions to occur is far less. Fig. 8 illustrates the experimental results.

4. Discussion

Following the early work of Tubandt, Jost and Wagner, polarization experiments with solid electrolytes are intensively studied and discussed.^{13,14,17)} It is the aim of this paper to draw attention to the possibility of electrically driven internal solid state reactions which are always based on oxidation or reduction processes. Let us refer to the following scheme of the galvanic cell under external load: $(+)\text{A}/\text{AX}(\text{B}_2\text{X}_3)/\text{AX}/\text{AX}(\text{C}_2\text{X})/\text{A}(-)$, the electrolyte AX of which is doped in such a way that with B_2X_3 dopant n-type conduction and with C_2X dopant p-type conduction is enhanced, see Fig. 9. Under electric load, and without decomposition, we have $j_A(\xi) = \text{const}$, which results in $\nabla\tilde{\varphi}(\xi) = \text{const}$ in the bulk phases. Since we assume that undoped AX is an ionic conductor with only a very small electronic transference, $j_h = -L_h(\nabla\mu_h + \nabla\tilde{\varphi})$ and $j_e = -L_e(\nabla\mu_e + \nabla\tilde{\varphi})$ must vanish everywhere. Therefore $\nabla\tilde{\varphi} = -\nabla\mu_h = \nabla\mu_e$, resulting in a decrease of μ_A near the anode and an increase near the cathode (note that $\mu_A^+ + \mu_e = \mu_A$; $\mu_A^+ = \mu_A + \mu_h$). The resulting overall course of the component potentials is schematically depicted in Fig. 9. The particular course in the undoped part of AX depends on the mobilities of h and e and on the relaxation times for their trapping and annihilation.

Applying these basic ideas to the ternary crystal (Mg, Fe)_{1-x}O brought between the two Pt-electrodes, we expect the following features to become visible: A zone (1) which exhibits a very low electronic conductivity near the cathode because of the following reasons: 1) The low oxygen potential near the interface (Mg, Fe)O/Pt(-) ensures that F_{Mg}^{2+} predominates. 2) If $D_{\text{Fe}}^{2+} > D_{\text{Mg}}^{2+} > D_{\text{Fe}}^{3+}$, Fe-ions are depleted in (Mg, Fe)O from a region near the cathode (zone (1)). 3) If $D_{\text{Mg}}^{2+} > D_{\text{Fe}}^{2+}$ new MgO will form near the cathode since the crystal is surrounded by an oxidizing gas. This newly formed crystal has been seen by electron microscopy. Zone (1) of low electronic conduction is clearly seen in all the

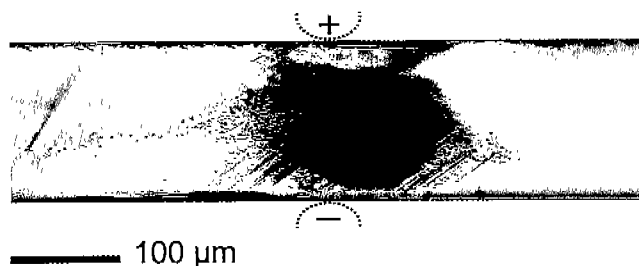


Fig. 8. Cross-section viewed by transmission optical microscopy; experimental conditions: $\log a_{\text{O}_2} = -8$, $T=900^\circ\text{C}$, $E=1.5 \text{ kV}\cdot\text{cm}^{-1}$, $x_{\text{FeO}}=1.2\cdot 10^{-2}$ and no preoxidation of the sample.

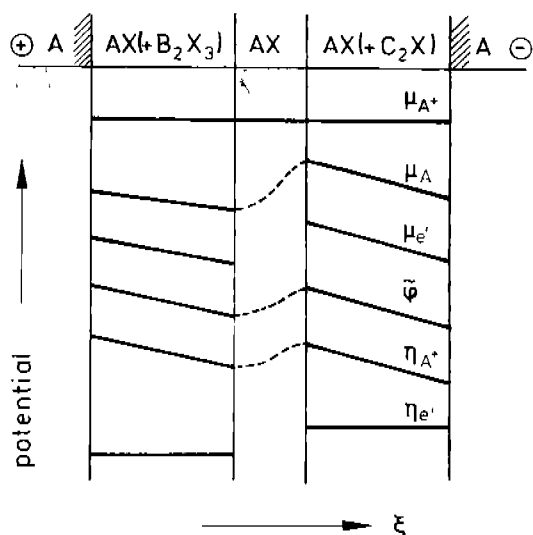
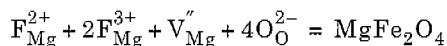


Fig. 9. Course of the various thermodynamic potentials in the galvanic cell Pt, X_2 /AX(+B₂X₃)/AX/AX(+C₂X)/Pt, X_2 under electric load (schematic). A=Mg, X=O, for example.

experiments, see Fig. 7.

In front of zone (1) towards the anode we have zone (2) with a higher oxygen potential and p-type conduction due to F_{Mg}^{3+} . Since $j_h = 0$ in view of the blocking of holes in the adjacent ionic zone (1) near the cathode, as discussed above ($\nabla_{\mu_h} \nabla_{\mu_o} - \nabla \tilde{\phi}$). When the oxygen potential, i.e. the electron hole potential in this zone has reached a certain limit, $MgFe_2O_4$ will precipitate according to the SE-reaction scheme.



and we note in passing that in view of the structure element reaction $O = O_O^{2-} + V_{Mg}'' + 2h^{\cdot}$, the chemical potential $\mu_O \sim \mu_h \sim \mu_{Fe}^{3+} \sim \mu_v$ in iron doped MgO. Zone (2) with spinel precipitates is found experimentally and is well illustrated for example in Figs. 6 and 7.

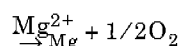
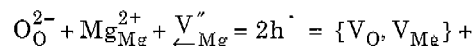
We note, however, that the slope of μ_O is positive in zone (2), which means that in this zone the oxygen potential is lowered towards to anode. This tendency must be reversed at some point near to the anode because eventually the highest oxygen potential is by necessity to be found near the anode.

We also observe that the spinel precipitates in zone (2) form preferentially at dislocations and decorate them. This agrees with earlier observations on other systems which undergo driven internal reactions.^{10,18)} Occasionally one can find the decorated lines to penetrate beyond zone (2) towards zone (1), indicating the dislocations to be high diffusivity paths for matter transport.

Zone (3), according to the former reasoning, has a lower oxygen potential than zone (2), although it is closer to the anode. In the early stage of the driven reactions this is due to the fact that the internal oxidation zone (2) has not yet sufficiently progressed. At the later stages, however, one has to take into account that if (Mg, Fe)O is oxidized, not

only spinel precipitates will form, but defect associates such as $(V_{Mg}'' Fe_{Mg}^{3+})'$ occur, which, in the internal electric field, migrate towards the anode. This may contribute to a depletion of Fe^{3+} in zone (3) towards the anode. In any case, the overall transport scheme in the different regions of the (Mg, Fe)O-crystalline solution may be quite complicate in view of these defect associates.²⁰⁾

Finally, zone (4) near the anode consists of porous material, and the iron ions are expected to exist in form of Fe^{3+} . The porosity stems from the morphological instability of the anodic interface.²¹⁾ The interface reaction is



and creates empty lattice molecules $\{ \}$ which cluster to form macroscopic pores that penetrate into the crystal. These pores along with an increase in Fe-concentration can be observed by analytical electron microscopy. Further details will be given in a forthcoming publication.²²⁾

5. Conclusion

Little work has been done yet concerning the influence of external driving forces on the combined reaction and transport behaviour of nonmetallic compounds and solid solutions. This is in particular true for systems with more than two components. Some work that concerns the spinel formation in this context can be found in.³⁾

A proper analysis of this influence requires some knowledge of the basic thermodynamics of the system including a valid phase diagram of the second kind.¹⁹⁾ With the help of this phase diagram one can at least obtain a qualitative notion of the reaction path. For ternary and higher systems these diagrams are often not available, if one or more components are metalloids.

We have demonstrated for the important ceramic system (Mg, Fe)O the implications to be expected if electrodes are attached and an external voltage is applied to the sample. In contrast to binary systems, the occurrence of internal reaction (oxidation and reduction) are the rule if only the applied voltage is sufficiently high.

If thermodynamic and kinetic properties of the electrodes and of the crystal under load are known, it is in principle possible to solve the transport/reaction problem unambiguously.

For (Mg, Fe)O it has been shown that an initially homogeneous crystal will become inhomogeneous under the action of the d.c. electric field. The subsequent local variations in the ionic and electronic transference numbers lead to a non-monotonic course of the oxygen chemical potential inside the crystal and a sequence of reducing and oxidizing zones, in which spinel formation takes place. The morphology of the samples in a quasi-steady state depends to some extent

on the oxygen potential of the surrounding atmosphere and the pretreatment of the (internally oxidized) sample.

Acknowledgements

I am indebted to the Deutsche Forschungsgemeinschaft and the Fonds der Chemischen Industrie for generous financial support and to S. Smolin for performing the experimental work.

Literature

1. H. Schmalzried, *Chemical Kinetics of Solids*, VCH Weinheim, 183 ff (1995).
2. T. Pfeiffer and H. Schmalzried, *Z. Phys. Chem. NF*, **161**, 1 (1989).
3. H. Schmalzried, W. Laqua, P. L. Lin and Z. Naturf., **34 a**, 192 (1975).
4. T. Grosse, Ph-D-Thesis, Universität Hannover, **34**, ff (1991).
5. C. Rosenkranz and J. Janek, *Solid State Ionics*, **82**, 95 (1995).
6. S. Yuan, M. Pal, *J. Electrochem. Soc.*, **143**, 3214 (1996).
7. A. V. Virkar, *J. Electrochem. Soc.*, **138**, 1481 (1991).
8. H. Schmalzried, *Chemical Kinetics of Solids*, VCH Weinheim, 177 ff (1995).
9. T. Pfeiffer *et al.*, *Ber. Bunsenges., Phys. Chem.*, **92**, 589 (1988).
10. U. Stikkenböhmer and H. Schmalzried, *Phys. Stat. Sol.*, **a146**, 31 (1994).
11. J. Janek and C. Korte, (unpublished).
12. D. Ricoult and H. Schmalzried, *J. Mater. Sci.*, **22**, 2257 (1987).
13. C. Wagner and Z. Elektrochem., **60**, 4 (1956).
14. T. Grosse and H. Schmalzried, *Z. Phys. Chem. N.F.*, **172**, 197 (1991).
15. J. Mizusaki *et al.*, *Bull. Chem. Soc. JPN.*, **48**, 428 (1975).
16. H. Schmalzried, *Ber. Bunsenges. Phys. Chem.*, **87**, 551 (1983).
17. M. H. Hebb, *J. Chem. Phys.*, **20**, 185 (1952).
18. U. Stikkenböhmer, Ph-D-Thesis, Universität Hannover (1994).
19. H. Schmalzried, A. Navrotsky, *Festkörperthermodynamik*, Verlag Chemie, Weinheim (1975).
20. M. Schröder and M. Martin, "Tracer Diffusion and Electrotransport in Indium-doped Cobaltous Oxide ($\text{Co}_{1-x}\text{In}_x$)_{1.5}O," *Diffusion and Defect Forum*, **143-147**, 1683 (1997).

REFERENCES

1. H. Schmalzried, *Chemical Kinetics of Solids*, 183-207, VCH, Weinheim, 1995.
2. T. Pfeiffer and H. Schmalzried, "Spinel Formation-A Detailed Analysis," *Z. Phys. Chem. NF*, **161**, 1-17 (1989).
3. H. Schmalzried, W. Laqua and P. L. Lin, "Crystalline Oxide Solid Solutions in Oxygen Potential Gradients," *Z. Naturforsch.*, **34a**, 192-199 (1979).
4. T. Grosse, Ph. D Thesis, Universität Hannover, 1991.
5. C. Rosenkranz and J. Janek, "Determination of Local Potentials in Mixed Conductors-two Examples," *Solid State Ionics*, **82**, 95-106 (1995).
6. S. Yuan and M. Pal, "Analytic Solution for Charge Transport and Chemical-potential Variation in Single-layer and Multilayer Devices of Different Mixed-conducting Oxide," *J. Electrochem. Socl*, **143**(10), 3214-3222 (1996).
7. A. V. Virkar, "Theoretical Analysis of Solid Oxide Fuel Cells with Two-layer, Composite Electrolytes:Electrolyte Stability," *J. Electrochem. Soc.*, **138**(5), 1481-1487 (1991).
8. H. Schmalzried, *Chemical Kinetics of Solids*, **117-123**, VCH, Weinheim 1995.
9. T. Pfeiffer, H. Schmalzried and Y. Ueshima, "Local Defect Equilibria-The Conceptual Difficulties in Treating Solid State Reaction Kinetics," *Ber. Bunsenges. Phys. Chem.*, **92**, 589-595 (1998).
10. U. Stikkenböhmer and H. Schmalzried, "Driven Internal Solid State Reactions-A Decoration Technique," *Phys. Stat. Sol.*, **146**(1), 31-41 (1994).
11. J. Janek, C. Korte, (unpublished).
12. D. Ricoult and H. Schmalzried, "Internal Reactions in the (Mg, Me)O System," *J. Mater. Sci.*, **22**, 2257-2266 (1987).
13. C. Wagner, "Galvanische Zellen mit Festen Elektrolyten mit Gemischter Stromleitung," *Z. Elektrochem.*, **60**, 4 (1956).
14. T. Grosse and H. Schmalzried, "Elektrochemische Untersuchungen an der Polarisationskette $\text{Al}/\text{AgBr}/\text{Pt}$," *Z. Phys. Chem. NF*, **172**, 197-208 (1991).
15. J. Mizusaki, K. Fueki and T. Mukaibo, "An Investigation of the Gebb-Wagner's d-c Polarization Technique I. Steady-state Chemical Potential Profiles in Solid Electrolytes," *Bull. Chem. Soc. Jpn.*, **48**, 428-431 (1975).
16. H. Schmalzried, "Internal and External Oxidation of Non-crystalline Compounds and Solid Solution (I)," *Ber. Bunsenges. Phys. Chem.*, **87**, 551-558 (1983).
17. M. H. Hebb, "Electrical Conductivity of Silver Surfide," *J. Chem. Phys.*, **20**, 185-190 (1952).
18. U. Stikkenböhmer, Ph. D Thesis, Universität Hannover, 1994.
19. H. Schmalzried and A. Navrotsky, *Festkörperthermodynamik*, Verlag Chemie, Weinheim, 1975.
20. M. Schröder and M. Martin, "Tracer Diffusion and Electrotransport in Indium-doped Cobaltous Oxide ($\text{Co}_{1-x}\text{In}_x$)_{1.5}O," *Diffusion and Defect Forum*, **143-147**, 1683 (1997).
21. M. Martin, "Transport and Degradation in Transition Metal Oxides in Chemical Potential Gradients," *Mater. Sci. Rep.*, **7**, 1-86 (1991).
22. S. Smolin, Ph. D Thesis, Universität Hannover (to be published).